SLAC-PUB-274
February 1967

SUPERCONDUCTING MAGNETS FOR HIGH ENERGY PHYSICS APPLICATIONS*

H. Brechna

Stanford Linear Accelerator Center
Stanford, California

ABSTRACT

With the availability of high energy accelerators the need for powerful experimental, beam transport and special magnets is steadily increasing. Experimental high field large volume watercooled or conventional magnets would have power requirements which would be economically unsound. Superconducting magnets have reached a stage where they can be incorporated in connection with high energy physics, and many laboratories are building experimental magnets to be used for charged particle energies between 10 and 20 GeV.

Recent developments in hard superconductors, technological improvements and a better understanding of steady state stable behaviour of superconducting magnets enables us to build multimegajoule energy magnets with fields approaching 100 kG in working values of several cubic meters. Recent trends in superconducting magnet design will be discussed. A number of large superconducting magnets currently in operation will be described as well as magnets in stages of procurement and planning.

The use of ferromagnetic materials with superconducting magnets, the effects of superfluid and supercritical helium in magnet performance and forced liquid helium cooling will be treated.

*Work supported by the U. S. Atomic Energy Commission.

(Presented at the International Cryogenic Engineering Conference, April 1967, Kyoto, Japan)

I. INTRODUCTION

Superconducting magnets have been considered in combination with high energy physics for several years. However, the areas where superconducting dc magnets were and are planned to be used are primarily in the experimental areas where the particle beam is fairly clean and the nuclear irradiation effects on the whole cryogenic system is considered less dangerous.

It was therefore logical to introduce superconducting magnets for bubble chamber experiments. However, for large superconducting systems to be used in high energy physics experiments, the initial cost, safety requirements, stability of operation and cool-down costs are quite a formidable problem. Thus, to consider and build large superconducting systems, the time element, as well as the understanding of the inherent properties of these systems required a long time prior to introducing them in combination with high energy physics experiments. The basic research of several laboratories in collaboration with industry made it possible for a 28 cm Helmholtz-type magnet to be built by Argonne National Laboratory for a 25.4 cm liquid helium bubble chamber. The system has been used successfully for a series of experiments at fields up to 40 kG.(1)

Encouraged by the better understanding of stabilized magnets, a number of laboratories(2, 3, 4, 5) are either planning or are in the construction phase of large superconducting magnets to be used in combination with 1 - 4 m diameter liquid hydrogen bubble chambers.

The designed field values are between 2 and 8 Vs/m^2. However, in other areas such as spark chamber and spectrometer work, liquid hydrogen targets, etc., the activity on superconducting magnets has been either non-existent or very slow.

In beam transport areas, considerable work has been done by Sampson, et al.,[6] where several quadrupole magnets on a basis of Nb_3-Sn ribbon with cylindrical geometry without ferromagnetic flux return paths were built and tested. It is reported that these quadrupoles had field gradients up to 7.5 kG/cm, and apertures up to 7.6 cm. Septier[7] reports on performance of a 5.2 cm aperture 6.8 kG/cm field gradient and effective length of 19.2 cm quadrupole lens with Nb-Zr multistranded cable and a non-ferromagnetic yoke for support of the coils. Superconducting magnets have been built for polarized target experiments[8] producing fields up to 25 kG in the bore with a field homogeneity of 10^{-4} over a sphere of 5 cm.

Hand in hand with the improvements in magnet technology and design techniques, coil optimization, improving magnet performance and its characteristics, controlling forces and stability, the performance of the basic hard superconductors such as Nb_3-Sn,[9] Nb-Ti[10] and Nb-Zr[11] have been improved considerably in recent years. As can be seen from Fig. 1 the field-current density characteristics of several hard superconducting alloys could be improved by using new cold work and precipitation heating techniques, as well as introducing ternary superconducting systems.

It was found,[12] that the H-J characteristic of Ti-Nb alloys is independent of size effects, as was observed in Nb-Zr alloys and thus the basic conductor-design was improved. Instead of using several small size wires (usually in the range of 0.025 cm diameter), one large superconductor can be used in the conductor. The maximum size of a superconductor used to present in a single line conductor has 0.2 cm diameter. Due to the poor heat conductivity of the superconductor at 4.2°K, Fig. 2, it is not clear that larger diameter superconductors may exhibit same properties. Superconducting strips[13,14] have inherently a better surface to area ratio and due to better cooling properties have been produced in large widths up to 1.3 cm and thickness of 0.05 cm on Nb_3-Sn and Nb-Ti basis used in solenoids with central fields up to 150 kG and 15 cm bore.[15] The introduction of stabilized conductors and cables on basis of copper cladding, and copper swaging or stranding with several copper or alunimun wires and using better impregnation alloys have made it possible for single conductors to carry several thousand Amperes without endangering the system due to sudden flux transitions or partial coil quenching. Instead of improving the conductor stability by adding more low electrical conductivity materials parallel to the bulk superconductor, other ways of improving the field shielding effect by making the conductor more porous,[16] or winding the coils in a rather open fashion[17] without jeopardizing the magnet strength, has been studied and utilized. Using materials with high thermal capacity and better heat conductivity at liquid helium temperatures compared to copper or aluminum have been investigated, to improve net current densities in magnets.

It may be pointed out that these progresses are indeed encouraging; however, the step to replace conventional dc magnets by superconductors in a large scale, to be utilized in high energy physics in combination with accelerators is far from being realized. It is too optimistic to predict the near future of dc magnets to be superconducting due to a number of difficulties which yet have to be investigated.

The performance of magnet systems for and in accelerators, where nuclear radiation hazards pervent a close supervision of the coil performance, must be investigated. It is not known what effect thermal neutrons or fast gammas will have on the coil, dewar and helium system, exposed to radiation and secondary particles. Although irradiation tests performed on Nb_3Sn and Nb-Zr indicate an improvement in the critical current density of the bulk superconductor.[18] Beam mis-steering may have disastrous effects and a failure, even if it is a partial quench of a single magnet for bending, focusing or steering of particle beams, may lead to a shutdown of the accelerator for several days and thus to an appreciable loss of time and money. However, for experimental magnets the present status of magnet technology permits the building of large scale superconducting dc magnets with or without ferromagnetic flux return paths and refrigeration system with appropriate safety features.

II. SUPERCONDUCTING EXPERIMENTAL SYSTEMS

Utilization of hard superconductors in dc magnets increases by an order of magnitude the field which could be economically achieved in conventional experimental, or beam transport magnets. This suggests many possible applications in elementary particle physics, particularly in systems involving high momentum charged particles, short path lengths and large divergence beams, which may be difficult or impossible to achieve with conventional magnets with iron flux return paths and normal conductor (Cu or Al) coils.

In this chapter, a comparative study of superconducting and conventional systems, such as bubble chamber, bending magnet and focusing system is made. The object of this study is:

1. Establish circumstances in which superconducting systems may become useful.
2. Determine whether the use of superconductors instead of conventional magnets, make any appreciable difference to the optimum choice of parameters.
3. Find whether superconducting coils might be a comparative alternative to conventional magnets.
4. Compare feasibility and safety of operation between superconducting and conventional magnets.

A simple and most realistic general picture is obtained by using approximate cost as the basis of comparison. This is because the magnetic fields which can be produced with superconductors may also be generated by conventional techniques. For the majority of high energy physics applications the criteria of practicability, convenience and cost are essentially the same.

It is tempting to take advantage of the high field properties of modern superconducting alloys and reduce the effective length of the gap according to the relation $\int B d\ell = \frac{p\Theta \cdot 10^7}{3}$ with p the particle momentum in GeV/c and Θ the deflection angle in radians. However, in many applications a lower limit of the chamber size, the magnet-end effects, fringing field patterns, and homogeneity requirements dictate the useful magnet volume even if higher fields may be attainable. Here are a few reasons:

1. The charged particles have a finite decay time. The decay may occur outside the chamber or in areas not accessible to photography.
2. Measurement accuracy may suffer due to loss of chamber resolution. The so-called vertical dip-angle of particles is independent of the magnetic field, the chamber resolution may be so poor that the chamber may prove to be inadequate.
3. The fringing field effect at high fields may effect the beam entry and exist, and constant values of $\int B d\ell$ or $\int \frac{dB}{dr} d\ell$ over the effective magnet length may be difficult to achieve in beam transport magnets.
4. Certain required field homogeneity in a useful experimental area may become a difficult problem to solve.
5. Forces may become exorbitant and set an upper field limit.

Compared to very large low-field chambers, medium or small size chambers with diameters around one meter and axial length of 0.5 meter operating at fields of 50-100 kG have a number of advantages. For example, reducing the gap diameter of a 2 m conventional experimental magnet of 20 kG by a factor 2 and increasing the transverse field by a factor of 4, which is in agreement with the $B\sqrt{\ell_{eff}}$ relation, leads to the following:

1. Photography of interactions is simpler.
2. Secondary electrons produced by particle beams in bubble chambers will produce at low fields large diameter tracks and complicate scanning. At high fields the electron track may be a dot on the film and thus less disturbing.
3. In bubble chambers, multiple scattering experiments are better to observe.
4. Reduction of smaller track fields (i.e., from 1m diameter to 35 mm or 70 mm film size) for scanning, is better without too much loss in measurement accuracy, than photographic reduction of large track areas.
5. In bubble chambers the triggering of the flashlight to the beam entry is performed by correlating chamber expansion to beam entry. Smaller chambers can be pulsed more frequently, which yields a better compilation of experimental data.
6. Photography of events are simpler and scanning more clear, than using fish-eye photography in order to photograph the whole useful chamber area. Measurements accuracy can be improved considerably.
7. Cost of auxiliary parts and buildings are reduced.

These few points cannot be generalized for all experimental magnets and a close cooperation between the experimental physicist and the magnet designer is essential to determine within the frame of possibility and practicability to determine the optimum size of the experimental area and field strength.

Prior to any cost studies it is necessary to outline the technical problematic of large high-field superconducting magnets in order to prepare the basis of comparison.

A. Technical Aspects of Large Stable Superconducting Magnets

Instead of talking in generalities, I will concentrate on three specific cases and study a 7 Vs/m^2, 1.3 m Helmholtz pair with ferromagnetic flux return path to be used either in combination with bubble or spark chambers, a bending magnet and focusing magnets. The parameters of the experimental magnet may seem far stretched, but it may be emphasized that several proposals are currently under study with parameters which are nearly alike or identical to the assumed numbers. The iron return paths are assumed asymmetric as illustrated in Fig. 3, to allow either photography (bubble chamber) from one side, or the ease in assembly and disassembly of chamber parts, counters, etc., in spark chambers.

B. Magnet Optimization

To compare the performance of the 1.3 m diameter and 7 Vs/m^2 superconducting magnet to a water-cooled conventional magnet which conveniently can produce a field of 2 Vs/m^2 we need a magnet diameter of 4 m. Using the computer code "Nutcracker"[(19)] for variable iron permeability, the conventional and superconducting magnets have been calculated and their basic parameters are given in Table I. In case of the superconducting magnet, ample space between the coils and the iron return path has to be provided to place the helium container, super-insulation and vacuum tanks, as well as support structures, in such a way as to withstand the axial and radial magnetic stresses.

High field coil requires for optimization a "grading" of the superconductor or current optimization. This means that the amount of superconductor in the wire, as well as the cross-section of the normal material, can be reduced for the same operational magnet current with lower fields over the coil area.

Subdividing the coil in several sections, axially and radially, will yield the same results with the additional advantage of limiting and reducing stresses produced by the magnetic field.

Based on current practices, high purity annealed copper was chosen as a substrate. Calculations in Chapter IV show that additional support means to improve conductor strength were necessary and are included in the comparison data.

In Table I, case (1) is a conventional 20 kG, 4 m diameter Helmholtz magnet. Case (2) is based on conventional practice of a superconductor embedded into a copper substrate by means of cabling or swaging (Fig. 4). Case (3) is calculated if hollow superconductors (Fig. 5) with internal helium cooling (supercritical) is chosen. The helium container is eliminated.

The conductor in case (2) is insulated by means of an open spiral wrapping of a braided and impregnated polyamid,[⊛] which provides the magnet with triangular-structured coolant passages.

C. Shubart-Type Bending Magnet

As basis of comparison, a bending magnet illustrated in Fig. 6 is considered. The bending magnet has a gap height of 36 cm and an effective length of 250 cm. The field at the wire is 20 kG yielding the value of $\int B d\ell = 5.25$ Vs/m. The gap height is determined by the experimental requirement and is not subject to any reduction. However, for superconducting conductors the field strength in the gap can be increased at least two-fold, which leads to a reduction of the effective length to 1.3 m. The magnet end-effects becomes more pronounced, but correcting the fringing fields by means of shimming is possible. Magnetic guard plates, or mirrors must be utilized. Table II compares the specifications of the conventional magnet to the superconducting magnet, where for this particular application hollow superconductors seem more adequate. The iron flux return path in the superconducting

[⊛] Trade name Nomex, Dupont, Distributor of braid: Westglas, San Francisco.

magnet had been increased adequately, although this would, if space requirements would be prohibiting, not be absolutely necessary. Ample space for the super-insulation, support structure, heat shields and vacuum tanks have been provided. Nitrogen shields would not be required, if the cold helium gas is conducted in such a way as to keep heat shields of various temperatures (between 20 and 80°K).

Bending magnets for higher transverse fields with iron return paths may be considered, but the utility of iron is rapidly diminishing at high fields due to saturation. The iron may serve merely as reinforcement, which will also contribute to the field in the gap.

D. <u>Superconducting Focusing System</u>

As mentioned above, quadrupole systems with <u>no</u> ferromagnetic flux return path system have been built and tested previously.[6, 7] The reason being the saturation of iron beyond 2.18 Vs/m^2, where the essential iron contribution to the focusing properties of the lens is lost. However, the iron may still be used around the coils providing structural strength and shielding the fringing field. Magnetic guard plates have to be provided to enhance end corrections. Study by Smith and Haskell[20] reveals that quadrupole systems may be compared by means of object to image distance ℓ for different combinations of Θ and p. Qualitatively, the cost of magnets in terms of ℓ may be presented in Fig. 7, where the cost of conventional magnets decrease with ℓ until the required fields at the pole tips reach $\left(1.5\text{-}2.2\right) Vs/m^2$. After this the benefit of iron from magneto-optical point of view is lost. Conventional quadrupoles are thus not used beyond pole tip fields of ~ 2.1 Vs/m^2 due to their excessive cost. However, superconducting quadrupoles with no iron or iron flux return path may be used up to peak fields of 15 Vs/m^2.

III. COIL STRUCTURES

The primary aim towards safety of operation is to make the coils stable against flux jumping for field changes. Stability can be achieved in several ways; one method is to provide a low electric conducting path parallel to the superconductor. Common practice is to use annealed high conductivity copper, or pure aluminum as substrates, which could carry parts of the current for some time in case of partial quenching. The low resistance path, which has to be in close electrical and thermal contact to the bulk superconductor serves several purposes:

1. It screens the field changes from adjacent turns and layers from individual conductors.
2. It provides a sink for joules heating generated by small flux jumps. The material is able to absorb the energy associated with these jumps without quenching. A simple limit of stability is obtained against thermal energy which can be absorbed instantaneously by the material.
3. In case of partial or complete quenches it will protect the superconductor and then the coil from complete destruction.
4. The transition from superconducting to normal condition is not instantaneous and the excessive helium boiling can be monitored by measuring the pressure build-up and the rate of gas leaving the dewars. Reducing the current to a recovery limit restores superconducting conditions.[21]
5. Phenomena in superconducting coils, observed in the early days of superconducting work, such as degradation, quenching at microscopic wire movements, Helmholtz-coil effects can be eliminated.

Combined with the use of a low resistance shunt the effect of cooling on stability is of great importance. It has been observed in many experiments that in so-called "well-ventilated" coils, where the coolant is in intimate contact with the superconductor and the substrate throughout the coil, the boil-off rate of helium during operations and the amount of helium necessary for cool-down from LN_2 temperature to $4.2^{o}K$ is drastically reduced.

In cases where turns were completely insulated electrically from each other the current change in the coil did depend only on the coil inductance, the external shunt resistance, and the power supply voltages. In coils with small inductances in the order of 10^{-2} Hy the magnet could be charged at a rate of more than 100 Amperes per second without appreciable changes in helium boil-off rate.

The cross section of the low resistance substrate surrounding the superconductor could be reduced with improvement of the heat transfer coefficient and thus resulted in a better net current density in the coil, or a higher space factor.

In current designs stability is achieved by a sacrifice in useful magnet volume. Space factors (ratio of superconductor to the coil cross section) attained, vary between 3-10% and at high transverse magnetic fields at the wire (say 7.0 Vs/m^2) the average current density does not reach 10^4 A/cm^2. It is therefore of interest to improve the average current density by means currently under investigation:

1. Increasing the contact area between superconductor and liquid or gaseous helium to improve the overall thermal capacity $(c_p \cdot \delta)$ of the system. Suggestions to produce a porous conductor is not recommended due to the high magneto-mechanical stresses in the coils.
2. Use of normal materials in conjunction to superconductors with high thermal capacity. Copper and aluminum prove to be poor in this respect. The use of indium as impregnant for copper or aluminum substrates improves the overall thermal capacity, but due to the poor mechanical strength was discarded. A combination of pure

tin and silver was used for impregnation and tinning which has tensile strength of 1,000 - 1,400 kg/cm^2 and has a specific heat value of $0.22 \cdot 10^{-3}$ Ws/g^oK (compared to $c_p = 10^{-4}$ Ws/g^oK for copper, $c_p = 0.28 \cdot 10^{-3}$ Ws/g^oK for alunimum, $c_p = 10^{-3}$ Ws/g^oK for indium, $c_p = 2 \cdot 10^{-3}$ Ws/g^oK for sodium and $c_p = 4.5$ Ws/g^oK for helium at saturation).

Sodium as substrate had been considered but was discarded due to poor mechanical performance.

The importance of improving thermal capacity of the structure can be seen readily from observations on two models, briefly mentioned below:

1. Thermodynamic Study State Model:

If we assume that the superconductor is somehow embedded in a normal material the solution of the study state thermodynamic equation(22) delivers:

$$\Delta T_n = K + (\Theta_c - K) \cdot e^{-mz} e^{(m^2+n)^{1/2} z} \qquad (1)$$

$$\Delta T_s = \Theta_c \cdot e^{-mz} e^{-(m^2+n)^{1/2} z} \qquad (2)$$

where Θ_c is the temperature difference between helium and critical temperature of the superconductor,

$$K = \frac{(i_n + i_s)^2 \cdot \rho_n}{h \cdot f \cdot A_s^{3/2}} \cdot \frac{1}{\left(\frac{\rho_n}{\rho_s} + \frac{A_n}{A_s}\right)\left(1 + \frac{A_n}{A_s}\right)^{1/2}} ,$$

$$m = \frac{c_{p_s} \cdot \delta_s}{2k_s} \cdot \frac{1 + \frac{A_n}{A_s} \cdot \frac{c_{p_n} \cdot \delta_n}{c_{p_s} \cdot \delta_s}}{1 + \frac{A_n}{A_s} \cdot \frac{k_n}{k_s}} \cdot v_q ,$$

$$n = \frac{h \cdot f}{k_s \cdot A_s^{1/2}} \cdot \frac{\left(1 + \frac{A_n}{A_s}\right)^{1/2}}{1 + \frac{A_n}{A_s} \cdot \frac{k_n}{k_s}} .$$

v_q is the speed of the quench front expressed as:

$$v_q = \frac{\sqrt{n}}{2} \cdot \frac{\frac{K}{\Theta_c} - 2}{\left(\frac{K}{\Theta_c} - 1\right)^{1/2}} \cdot \frac{2k_s}{c_{p_s} \cdot \delta_s} \cdot \frac{1 + \frac{A_n}{A_s} \cdot \frac{k_n}{k_s}}{1 + \frac{A_n}{A_s} \cdot \frac{c_{p_n} \cdot \delta_n}{c_{p_s} \cdot \delta_s}} \tag{3}$$

In non-superconducting state the resistivity of the normal material is much smaller than that of the superconductor,[22] $\rho_n \ll \rho_s$, and K can be modified to:

$$K = \frac{2(i_n + i_s)^2 \rho_n}{h \cdot A_n \cdot S} \tag{4}$$

In stable performance the quenching speed at a point $z = z_o = 0$ must be zero which means from Eq. (3) that $K = 2\Theta_c$ or:

$$(i_n + i_s)^2 \rho_n = h A_n \cdot S \cdot \Theta_c, \tag{5}$$

as a stability criteria relating the total current flowing through the composite winding to the heat transfer coefficient and the conductor geometry. However, we can see from Eqs. (1) or (2) that $\Delta T_n = \Delta T_s = \vartheta_c$ the critical temperature difference at a coordinate point $z = z_o$ and specifically at $z = 0$, if $m = 0$

or $m \gg 1$. $m = 0$ is accomplished with $v_q = 0$. $m \gg 1$ is possible only if:

$$A_n \cdot c_{p_n} \cdot \delta_n \gg A_s c_{p_s} \delta_s \quad .$$

For $A_n \cong A_s$ we see that the thermal capacity of the normal material must be much higher than that of the superconductor, to achieve stability.

The heat capacity of Nb_3-Sn has been measured by several authors[23] at 4.2^oK to be: $1.32 \cdot 10^{-2}$ Ws/cm^3 ^oK, and its specific heat: $3.4 \cdot 10^{-4}$ Ws/gr^oK. The specific heat for Nb (25%) Zr was measured by Bindari to be $1.8 \cdot 10^{-4}$ Ws/gr^oK. The heat capacity of liquid helium is thus about 340 times higher than for Nb_3-Sn and 550 times higher than Nb (25%) Zr. The simple comparison in heat capacity emphasizes the effect of cooling with liquid helium.

2. Field Screening Model:

Hancox[24] has shown with a simple one-dimensional model of Nb_3-Sn, that the total field which can be screened is limited to:

$$H_s \leqq (8\pi \, c_p \cdot \delta \cdot T_o)^{1/2} \tag{6}$$

where T_o is the characteristic temperature, defined by the ratio:

$$\frac{J_c}{T_o} = \frac{dJ_c}{dT} \quad ,$$

the change of critical current density as a function of temperature. Equation (6) shows that the field which may be screened is independent of the critical current density of the material (the higher the current density, the smaller the depth to which flux may penetrate before instability occurs), and also indicates that the screening is determined by the heat capacity $c_p \delta$ of the conductor material.

Various coil designs with nucleate liquid helium boiling provide cooling channels by means of axial, or radial spacings, around the superconducting-normal material conductor. Possible solutions are outlined in Fig. 4.

The insulation thickness around the conductor should be sufficient to prevent inter-turn, and most important, inter-layer shorts. However, the helium gap produced by the spiral insulation wrapping should have a hydraulic diameter which permits ready flow of helium, and prevents trapping of helium gas bubbles produced in the channels.

According to measurements of McInturff(17) the minimum gap height should be about 0.015 cm. The heat transfer coefficient measured at SLAC in coils with 7 cm i.d., 19 cm o.d. and 20 cm length energized with 700 Amperes dc having open structure with spacing between turns of 0.03 cm was 0.4 W/cm^2 max; the temperature gradient from the conductor surface in contact with He to the embedded superconductor is approximately $0.7\,^{\circ}K$ which gives a value of $h = 0.57\ W/cm^2\,^{\circ}K$. Only when the helium gaps between adjacent turns exceed 0.15 cm heat transfer values of $0.9\ W/cm^2\,^{\circ}K$ can be obtained.

The insulation material most adequate for wrapping around superconductors was found to be a polyamid braid composed of many filaments. Its great advantage compared to glass-filament braids is less brittleness and thus it does not fracture during wrapping. If impregnated with suitable impregnants, or adequately heat treated, it is only slightly affected by moisture, retains its dimensional stability under severe compressive stress, and did withstand cyclings between room and liquid N_2 temperatures when exposed to compressive stress of more than 9,000 kg/cm^2. Some of the mechanical properties of this polyamid braid (Nomex) are given in Table III.

A. Improvement of Heat Transfer

In above section stability limited by normal material was discussed at the nucleate boiling regions, where in the thermodynamic model transition and recovery currents were independent of the superconducting critical temperature. Operation in this region takes advantage of increased cooling by means of open-structured coils to support higher stabilized currents. We observed that the heat transfer coefficient may be doubled if the coolant gap height is increased by a factor of four over minimum recommended gaps of 0.025 cm.

Maximum heat flux of approximately 1 W/cm^2 can be removed at nucleate boiling regions if the temperature gradient in composite conductor between the superconductor and the outer conductor surface in contact with helium is nearly 1°K. At higher temperature gradients film boiling will occur where the heat transfer flux is reduced to small numbers down to 0.08 - 0.1 W/cm^2. It is conceivable to improve the film boiling heat transfer flux by using a thin insulation film with relatively good heat conductivity around the conductor. But this reduces the effect of nucleate boiling considerably. Some optimum value may be obtained by proper choice of parameters.

Another approach first tested at SLAC in 1965 and reported in 1966[22] was the use of forced liquid helium, either by means of pressurizing liquid helium through the coil or use of supercritical helium.

Three possible ways were considered:

1. The coil is built such that the liquid helium is forced to penetrate the coil at one radial face and leave it at the other face. The speed of helium passing between adjacent conductors is limited to a few cm/sec due to complex matrix of the coolant passages, and high friction losses. The advantage of the system is to remove any gas bubbles trapped in the coolant passages, and thus leading to hot spots, as well as improve the heat transfer slightly.

2. The superconductor is buried in the substrate, which is provided with a cooling hole for liquid helium passage. Various schemes studied up to present, are illustrated in Fig. 5.

To discuss properties of the hollow superconductor we consider a conductor with a hydraulic diameter of 0.3 cm. The length of one hydraulic passage, for the magnet described in Table I is 150 meters. With a pressure difference between entrance and exit of each passage to the 10 kg/cm^2 we get helium speed of $v = 3.0\ \mathrm{m\ sec}^{-1}$ corresponding to a Reynolds number of $Re = 5.1 \cdot 10^5$.

The heat-transfer coefficient for single phase flow is given by the correlation formulae:

$$\frac{hd_h}{k_\ell} = C \left[\frac{d_h \cdot \delta \cdot v}{\eta}\right]_\ell^{0.8} \left[\frac{c_p \cdot \eta}{k}\right]_\ell^{0.4} \tag{7}$$

The factor C for water was determined by MacAdams[25] to be $2.1 \cdot 10^{-2}$, SLAC measurements for single phase helium indicates a $C \cong 4 \cdot 10^{-2}$. By using the data from cryogenics handbooks[26] we get from Eq. (7) for liquid helium:

$$h = 0.86\ \mathrm{W/cm^2\ {}^oK}$$

If Eq. (7) is modified for nucleate boiling the heat-transfer coefficient will be more than doubled. However, since measurements are not terminated we will operate presently with $h \cong 0.8\ \mathrm{W/cm^2\ {}^oK}$ as a comparison value to data obtained for nucleate boiling.

If we assume that annealed high purity copper has been used as substrate, and we base our calculations on a square conductor with the dimensions of $0.635 \cdot 0.635$ cm we get the maximum limit of stable current through the magnet from Eq. (5):

$$I^2 = \frac{hAS}{\rho} \cdot \Delta T$$

For this particular conductor with superconductors embedded on the outer surface $\Delta T \cong 0.90^o$ K. The maximum field at the conductor is $7.6\ \mathrm{Vs/m^2}$ and thus the resistivity of copper is expressed as:

$$\rho = \rho_{o,\,273^oK}\left[\frac{0.9}{\frac{\rho_{o,\,273^oK}}{\rho_{o,\,4.2^oK}}} + 0.25\ B\cdot 10^{-2}\right] \tag{8}$$

$$= 4.4 \cdot 10^{-8}\ \text{ohm}\cdot\text{cm}$$

B is expressed in Vs/m^2. The empiric Eq. (8) yields higher values than one would obtain from Kohler diagram for copper.

With $A = 0.25\ cm^2$ $S = 1.0\ cm^2/cm$, we get: $I_{max} \cong 2.0 \cdot 10^3$ Amp.

At the inner section four conductors are connected in parallel and thus the 5,000 Amps operational current was selected in Table I. The average current density at the inner coil section with an insulation thickness of 0.03 cm each side of the conductor is $2.5 \cdot 10^3\ A/cm^2$. The coil is subdivided radially into three sections, where according to the maximum field at the conductor the number of parallel electrical currents is reduced from 4 to 3 and 2 carrying 5,000 Amps. The average coil current density is thus: $3.5 \cdot 10^3\ A/cm^2$.

For this solution the need for a helium container is eliminated. Each coil section can be impregnated in suitable thermosets and by providing superinsulation around the coil, confined by a vacuum jacket,maximum space between the surrounding iron and coil can be utilized. The design with hollow superconductors is specifically of interest in beam transport magnets, where the coils may be placed inside iron frames or yokes, thus protecting the magnet from irradiation hazards.

3. Operating magnets with sub-cooled helium below λ- point. Although this method seems very attractive and improves specifically in Nb_3-Sn wound coils to the upper critical current, its technical realization for large magnets is somewhat doubtful. Measurements at Brookhaven National Laboratory[27] with Nb_3- Sn indicate that the upper critical

field of solenoids with (2.5-5) cm bore could be increased by more than 30%. This improvement is due to the super-fluid character of the helium, which penetrates between layers in completely insulated coils and provides better cooling, as well as improves thermal capacity of the system. However, the improvement of the upper critical field in Nb-Ti coils wound in open structure is small, and does not justify the additional cost of pumping systems, although the recovery current was improved by more than 50%.

IV. STRESSES

The mechanical strength of the conductor imposes an upper limitation on the performance of high field magnets. The mechanical stress analysis based on interaction of Lorentz body forces throughout the winding structure shows that in coils with o.d. to i.d. ratios of $\geqq 2$, the peak stress in mechanically homogeneous coils is more severe than in decoupled, radially and axially regionalized coils. Due to the high current density in superconducting coils the limitations of the coil performance is primarily due to stresses and thus accurate stress calculations are required. Ways and means must be found to limit, or compensate the stresses. The calculations of stress distribution also reveal that the average current density in the coil should be inverse proportional to the field distribution over the coil. Fortunately, this requirement is also true for current optimized coils. Thus the current density of coils may be varied according to the coil stability from relative low values at the inner radius, to high values at the outer coil radius corresponding to the field distribution in the coil, as well as the maximum stable current carried by the conductor.

To relate Lorentz forces to the field and current distribution the axial and radial field distribution in the coil should be known. With available computer codes the field distribution can be calculated in any desired accuracy for a fine mesh.

The axial field in terms of the maximum field can be expressed as:

$$B_z = B_m \left[y - m \left(\frac{r}{a_1} - 1 \right) \right] \tag{9}$$

with

$$m = \frac{B_z(r)}{B_m} \qquad y = \frac{B_m}{B_{z(r=a_1)}}$$

The radial force in terms of body forces is given by:

$$dF_r = \frac{dF}{dV} \; rdr \; d\phi dz$$

with

$$\frac{dF}{dV} = \frac{B_m^2}{4\pi \cdot 10^{-7}} \cdot \frac{\left[y - m \left(\frac{r}{a_1} - 1 \right) \right]}{a_1 \; (\alpha - 1)} \tag{10}$$

The stress differential equation on a volume element rdr $d\phi dz$ may be given by:[28]

$$\sigma_t - \sigma_r - r \frac{d\sigma_r}{dr} - r \frac{dF}{dV} = 0 \tag{11}$$

This equation can be calculated by using the displacement equations. If we assume for simplicity that the coil axial displacement is constant, we may write for the tangential and radial stresses in Newton/m^2 :

$$\sigma_t = \frac{B_m^2}{96\pi(\alpha-1)(\mu-1) \cdot 10^{-7}} \left\{ A - B \frac{(1-2\mu)}{\gamma^2} + 8\gamma \; (y+m)(1+\mu) - 3m\gamma^2 (1+2\mu) \right\}, \tag{12}$$

$$\sigma_r = \frac{B_m^2}{96\pi(\alpha-1)(\mu-1) \cdot 10^{-7}} \left\{ A + B \frac{(1-2\mu)}{\gamma^2} + 8\gamma \; (y+m)(2-\mu) - 3m\gamma^2 (3-2\mu) \right\} \tag{13}$$

where

$$A = -8y(2-\mu)\left(1+\frac{\alpha^2}{\alpha+1}\right) + m\ (7-2\mu)\ \frac{1}{\left(\alpha^2-1\right)} - \frac{m\alpha^2}{\left(\alpha^2-1\right)}\left[8\alpha(2-\mu) - 3\alpha^2(3-2\mu)\right] ,$$

$$B = \frac{\alpha^2}{\left(\alpha^2-1\right)\left(1-2\mu\right)} \cdot \left\{ 8y(2-\mu)(\alpha-1) - m\left[(7-2\mu) - 8\alpha(2-\mu) + 3\alpha^2(3-2\mu)\right] \right\} ,$$

and

$$\gamma = \frac{r}{a_1} .$$

For example we calculate the maximum values of radial and tangential stresses for the 7 Vs/m^2 magnet specified in Table I.

For the inner section:

$$\alpha_i = 1.4$$

$$y_i \cong 1$$

$$m_i = 0.60$$

$$\mu = 0.33 \text{ (Poisson's ratio)}$$

we get:

$$A = -26.4; \quad B = +26.5$$

The maximum radial stress occurs at $\gamma = 1.155$ where $\sigma_r = 177\ kg \cdot cm^{-2}$.

The maximum tangential stress occurs at $\gamma = 1$ where $\sigma_t = 1{,}500\ kg \cdot cm^{-2}$. The tangential stress is beyond the yield strength of annealed copper at liquid helium temperature. Even if 8% of the conductor area is occupied by the superconductor, some reinforcements by means of stainless steel strips combined with the superconductor must be used to prevent the copper from cold work. The knowledge of the radial field distribution makes it possible to calculate the axial stresses, which in this case is $\sigma_a \cong 400$ kg/cm^2.

V. ECONOMICS

Having established main design features of high field superconducting magnets to be used for high energy physics applications we base the price comparison on "capital cost" rather than the "ten-year cost." This is because the former seems to be of greater interest and because the operating cost is somewhat uncertain for superconducting magnets in intermittent experimental use.

The economics study based on actual experience may lead to cost comparison between superconducting and conventional magnets. However, as mentioned in Chapter II prior to any economics study the physics requirements should be studied.

In most cases it is desirable to use iron, surrounding the coils, even if its contribution is small and the iron is saturated. New design practices and ideas change, of course, completely the basic price study. Any economics study is confined to different countries and generalization may have only academic value.

It is feasible to compare each type of magnet separately, but this would be beyond the scope of this report. Enough experience is now available to make a thorough cost analysis for each individual conventional magnet type. In large superconducting magnets, due to lack of experience the cost of winding, assembly, joints, dewars and auxiliary parts, which still are in a Taylor-made stage, are high. Only very few manufacturers have had any experience at building large superconducting magnets,[21] and thus the basic work has been performed by high energy laboratories. Even if we would compare under these circumstances, hardware costs of superconducting magnets and refrigeration system there is still an uncertainty factor which is quite hard to determine and may very well exceed the value of 2.

Detailed studies carried out in specific cases show that the capital cost of superconducting magnets and refrigeration system for similar fields multiplied by the useful volume is less than for conventional magnet, power supply system. An economics study for focusing magnets has been done in detail by Smith and Haskell.[20] Instead now of treating the economics study in detail, a cost comparison for the magnets according to Table I are given in Table IV.

In case of the hollow superconductor the price of producing the optimum design is still guess-work. For a possible design, illustrated in Fig. 5, the price of hollow superconductor, reinforced and insulated, is estimated at 7/m. The cost of refrigeration systems is based on current evaluations.

VI. SAFETY OF OPERATION

Due to the fact that the superconducting magnets to be used in high energy physics will have energies exceeding multimegajoules, a sudden quench may prove to be disastrous. The first step, of course, is to build the magnet stabilized such that prior to a quench the transition from superconducting to normal condition will be over a mixed stage and that the transition does not occur instantaneously. Thus, only fractions of the field energy will be converted to joules heating in the conductor, and current reduction to the limit of superconducting recovery may restore superconducting conditions. In case of large $\frac{dI}{dt}$ fluctuations or a power failure the magnet may quench. However, calculations backed by experimental evidence show that even with complete lack of liquid helium in stabilized coils the temperature rise may be very well kept below $400^{\circ}K$. General design trends prefer water-cooled shunts parallel to the magnet, which can absorb 5 - 10% of the dissipated field energy. Its advantage being keeping surge voltages during current fluctuations to a designed value.

In order to keep a complete record of hazards, occurring in superconducting magnets, several helium-level gauges, sensing leads across each layer, pressure monitors and flow meters should be provided. In many cases, where no iron return path is foreseen, a steel ring should be provided around the coil which may act as a short circuited secondary transformer winding absorbing the energy. A circuit to obtain slow and smooth field increase in superconducting magnets, as well as to protect the magnet is given in Figs. 8a and 8b.

Operating the magnets from a set of batteries which are continuously charged is advisable. In case of power failures, $\frac{dI}{dt}$ can be kept at a rate which prevents coil quenching.

VII. LABORATORY MODEL TESTS

In this chapter we briefly mention the installations at SLAC to study and if necessary wind and assemble large superconducting magnets. At present we are building a 30 cm, 75 kG superconducting Helmholtz-type magnet, which may serve various experimental purposes, as well as to help study the inherent characteristics of large coils. Figure 9 illustrates the magnet parameters. The magnet is wound in six sections where Table V shows the magnet specifications. The four inner coil sections have been tested and the voltage current oscillograms is given in Fig. 10. The magnet installation is shown in Fig. 11 and the refrigeration system including the magnet inner sections is given in Fig. 12.

VIII. CONCLUSIONS

Although the advancements of superconducting work as such are quite rapid, it has only been used in large bubble chamber magnets and is investigated in magnetic lenses and bending magnets. However, new designs and reliable materials capable of carrying 10^5 A/cm^2 above 50 kG fields widen the economics, as well as open new experimental possibilities, not feasible with the aid of conventional dc magnets. It is obvious that the earlier applications of superconductors is in the high dc magnetic field. Applications in ac and microwave systems are under investigation, but it is too early to predict the use of hard superconductors in accelerators.

REFERENCES

1. M. Derrick, et al., "The Argonne National Laboratory-Carnegie Institute of Technology 25-cm Bubble Chamber Superconducting Magnet System," Proc. 1966 International Conference on Instrumentation for High Energy Physics, Stanford Linear Accelerator, Stanford, California; p. 264.

2. "Proposal for the Construction of a 12-Foot Liquid Hydrogen Bubble Chamber," Argonne National Laboratory, Argonne, Illinois (June 10, 1964).

3. "Proposal for the Construction of a Cryogenic Bubble Chamber of 14-Foot Diameter for use at the Brookhaven Alternating Gradient Synchrotron," Brookhaven National Laboratory, Physics Department, Upton, New York (Rev. June 1965).

4. "Report on the Design Study of a Large Hydrogen Bubble Chamber for the CERN Proton Synchrotron," CERN TC/BEBC 66-73, CERN, Geneva, Switzerland (October 1966).

5. J. Ballam, et al., "Proposal for the Construction of a 1.30 m, 70 kG Superconducting Liquid Hydrogen Bubble Chamber Magnet," Stanford Linear Accelerator, Stanford, California (in preparation).

6. P. G. Kruger, W. B. Sampson, R. B. Britton, "A Superconducting Quadrupole Lens," Brookhaven National Laboratory Report No. AADD-104 (March 30, 1966).

7. A. Septier, J. C. Molza, L. Donadieu, "Realization of an Iron Free Super-Conducting Quadrupole Lens, "IEEE Trans. on Magnetics, Vol. Mag-2, 326 (September 1966).

8. H. Desportes, "Aimant CPB Characteristique Provisoires," Departement de Physique des Particules Elémentaires, Internal Report, Saclay, France (private communication).

9. "Complimentary Ribbon for RCA Commercial Types SR 2100 and SR 2101," RCA R-60291, 8-66, New "Vapodep" Niobium-Tin Superconductive Ribbon, RCA, New York, New York 10020.

10. "Stabilized Superconducting Materials," Atomic International, Canoga Park, California.

11. J. Wong, Supercon Div. of N.R.C., Natwick, Massachusetts, private communication.

12. A. D. McInturff, et al., H. Brechna, et al., "Size Effect and Critical Transport Current in Titanium (22 at % Niobium)," SLAC PUB 220, Stanford University, Stanford, California (October 1966).

13. C. Laverick, "Superconducting Magnet Systems," Argonne National Laboratory, October 3-6, 1966.

14. M. G. Benz, "Superconducting Properties of Diffusion Processed Niobium-Tin Tape," G. E. Internal Report, General Electric, Schenectady, New York.

15. E. R. Schrader and P. A. Thompson, "Use of Superconductors with Varied Characteristics for Optimized Design for Large-Bore High-Field Magnets," IEEE Trans. on Magnetic, RCA Publ. No. ST 3149 (September 1966).

16. R. Hancox, "Stability Against Flux Jumping in Sintered Nb_3-Sn," Phys. Letters 16, 208 (June 1965).

17. A. D. McInturff, Private communication.

18. G. W. Cullen and R. L. Novak, "Effect of Neutron Induced Defects on the Current Carrying Behavior of Vapor Deposited Niobium Stanide," Appl. Phys. 37, 3348-3352 (August 1966).

19. E. A. Burfine, L. R. Anderson, H. Brechna, "A Computer Code for Variable Permeability Magneto-Static Field Problems," SLAC Report 56, Stanford, California (April 1966).

20. P. F. Smith and G. P. Haskell, "Superconducting Focusing Systems in High Energy Physics," Nucl. Instr. and Meth. 43, 285-297 (1966).

21. Z. J. J. Steckly, et al., "A Large Experimental Superconducting Magnet for MHD Power Generation," VI-I Avco Everett Res. Lab., Everett, Massachusetts (June 16, 1966).

22. H. Brechna, "A High Field 1.3 m Superconducting Split Coil Magnet with Forced Liquid Helium Cooling," SLAC PUB 182, Stanford, California (April 1966).

23. A. E. Bindri and M. M. Litvak, "The Upper Critical Field of Nb-Zr and Nb-Ti Alloys," Avco-Everett Research Laboratory, BST-TDR-63-62, AMP 101, January 1963.

24. R. Hancox, "The Superconductivity of Sintered Nb_3-Sn at Temperatures above 4.2^{o} K," Appl. Phys. Letters 7, No. 5 (September 1965).

25. W. H. McAdams, Heat Transfer, (McGraw-Hill Book Company, New York, 1954).

26. National Bureau of Standards, Properties of Materials at Low Temperature, Phase I, A Compendium, Edited by V. J. Johnson (Pergamon Press, 1961).

27. W. B. Sampson, Brookhaven National Laboratory (private communication).

28. H. Brechna, "Insulation Structure and Coil Reliability," Proc. Intern. Symp. on Magnet Technology, Ed. H. Brechna, H. S. Gordon, Stanford Linear Accelerator Center, Stanford, California (1965), p. 321.

TABLE I

COMPARISON BETWEEN EQUIVALENT WATER-COOLED AND SUPERCONDUCTING EXPERIMENTAL MAGNETS

MAGNET PARAMETERS	20 kG (WATER-COOLED)	70 kG (HOLLOW SC)	70 kG (CABLE SC)
a_1	200 cm	68 cm	73 cm
α	1.5	1.8	1.78 cm
β_{left}	0.25	0.26	0.25
β_{right}	0.25	0.3	0.3
2g	36 cm	40 cm	45 cm
γ_1	0.34	0.56	0.56
γ_2	0.34	0.62	0.617
I	10,000 Amp	5,000 Amp	5,000 Amp
N_{left}	400	1,350	1,580
N_{right}	400	1,670	1,950
Series Turns per layer (left)	20	13/17/26	13/17/26
Series Turns per layer (right)	20	16/21/32	16/21/32
Number of Layers	20	$3 \cdot 24$	$3 \cdot 24$
Cond. Dimensions Bare	$4.8 \cdot 4.8$ cm^2	$0.635 \cdot 0.635$ cm^2	$0.6 \cdot 0.6$ cm^2
Parallel Turns	---	4/3/2	4/3/2
Total Amp Turns	$8 \cdot 10^5$ At.	$15 \cdot 10^6$ At.	$17 \cdot 10^6$ At.
Average Current Density	$6.25 \cdot 10^2$ A/cm^2	$3.5 \cdot 10^3$ A/cm^2	$3.8 \cdot 10^3$ A/cm^2
Number of Parallel Hydr. Passages	4	4/6/8	---
Length of Hydr. Passage	250 m	130/110/120m	---
Diameter of Cooling Passage	3 cm	0.3 cm	---
Cu-Weight	$180 \cdot 10^3$ kg	$15.5 \cdot 10^3$ kg	$16 \cdot 10^3$ kg
Supercond. Weight	---	$1.1 \cdot 10^3$ kg	$\sim 1.1 \cdot 10^3$ kg
Magnet Energy	$\sim 70 \cdot 10^6$ joules	$60 \cdot 10^6$ joules	$70 \cdot 10^6$ joules
Charging Voltage	1,600 Volts	30 Volts	30 Volts
Charging Time	9 Sec.	850 Sec.	1,000 Sec.
Power Requirement (Charging)	$16 \cdot 10^6$ W	$2.15 \cdot 10^5$ W	$2.15 \cdot 10^5$ W
Heat Losses in Coils (4.2°K)	---	98 Watts	100 Watts
Refrigeration Requirement (300°K)	---	~100 kW	~100 kW

TABLE II

COMPARISON BETWEEN EQUIVALENT WATER-COOLED AND SUPERCONDUCTING BENDING MAGNETS

MAGNET PARAMETERS	20 kG (Water-Cooled)	40 kG (Supercond)
Gap Height (m)	0.36	0.36
Gap Width (m)	0.46	0.46
Effective Length (m)	2.5	1.30
Total Amp-Turns	$7.36 \cdot 10^5$ At.	$1.5 \cdot 10^6$ At.
Oper. Current (Amp)	2,630	2,000
Number of Turns per Coil	140	376
Number of Coils	2	2
Conductor Dimensions (cm^2)	$2.28 \cdot 1.65$	$0.55 \cdot 0.55$
Cooling Passage Diameter (cm)	1.111	0.3
Average Current Density ($A \cdot cm^{-2}$)	$9.45 \cdot 10^2$	10^4
Weight of Cond. Material (kg)	$7.8 \cdot 10^3$	$6 \cdot 10^2$
Weight of Iron (kg)	$35 \cdot 10^3$	$20 \cdot 10^3$
Power Requirement (Watts)	$950 \cdot 10^3$	$24 \cdot 10^3$
Magnet Price ($)	$100 \cdot 10^3$	$60 \cdot 10^3$
Power Supply Price ($)	$50 \cdot 10^3$	$4 \cdot 10^3$
Refrigerator Price ($)	---	$40 \cdot 10^3$
Helium Dewar Price ($)	---	$15 \cdot 10^3$
Auxiliary Price ($)	---	$10 \cdot 10^3$
Total Price (Magnet System) (U.S. $)	$160 \cdot 10^3$	$129 \cdot 10^3$

TABLE III

PHYSICAL PROPERTIES OF INSULATION FILAMENTS TESTED AT 78°K [1]

PROPERTIES	INSULATION		
	Glassfibre [2] Epoxy - Silicone	Polyester (monofilament)	Polyamid [3] Heat Treated-Silicone
Tensile Strength ($kg\ cm^{-2}$)	$3 \cdot 10^4$	$5.7 \cdot 10^3$	$4 \cdot 10^3$ (2% elongation)
Breaking Elongation (%)	<1	11	8
Initial Modulus ($kg\ cm^{-2}$)	$8 \cdot 10^5$	$7 \cdot 10^4$	$2.6 \cdot 10^5$
Compressive Strength ($kg\ cm^{-2}$)	$2 \cdot 10^4$ $2.6 \cdot 10^4$	$(3.5 \ldots 7.6) \cdot 10^3$	$(6 \cdot 10^3 \ldots 1.2 \cdot 10^4)$
Specific Heat (Ws/g^oK)	0.4	0.6	0.7
Heat Conductivity (W/cm^oK)	$3 \cdot 10^{-3}$	$1.2 \cdot 10^{-3}$	$1.1 \cdot 10^{-3}$
Specific Gravity ($gr \cdot cm^{-3}$)	2.55	1.1 - 1.4	1.3

1. The mechanical properties are average values of 5 samples. Values fluctuate ±30.
2. Glassfibre braids are impregnated either with epoxies, or silicones as binders. They do not lose their elastic properties.
3. Also called Nomex Nylon.

TABLE IV

COST COMPARISON BETWEEN CONVENTIONAL AND SUPERCONDUCTING EXPERIMENTAL MAGNET. (MAGNET PARAMETERS IN TABLE I)

MAGNET PARAMETERS	COST IN 10^6 U.S. DOLLARS		
	20 kG (WATER-COOLED)*	70 kG (HOLLOW SC)	70 kG (CABLE SC)
Coils Installed	1.0	0.6	0.5
Return Yokes	0.50	0.15	0.15
Power Supply and Regulation	0.60	0.03	0.03
Magnet Transport System	0.15	0.08	0.08
Safety Gadgets	0.02	0.05	0.05
Vacuum System	--	0.2	0.30
Refrigeration System	--	0.4	0.5
Miscellaneous	0.05	0.1	0.1
Total	2.32	1.61	1.71

* In the cost comparison, the additional cost of pumps, water tower, water piping have not been included as they are standard equipment in high energy laboratories.

TABLE V

SLAC 30.5 cm, 75 kG HELMHOLTZ COIL

Coil Section	a_1 (cm)	α	$\beta^{(1)}$	$N^{(2)}$	J_{av} $(A.cm^{-2})$	B_{max} at cond. (Vsm^{-2})	Space Factor[3] (%)
Inner	15.25	1.75	0.96	5,000	$3.36 \cdot 10^3$	8	12.5
Middle	27.25	1.165	0.537	2,800	$4.84 \cdot 10^3$	4.7	10
Outer	32.4	1.385	0.45	5,200	$3.16 \cdot 10^3$	2.6	5

---

1. β - for each half section.
2. N - Turns for both half sections.
3. Are average values. S.C. are graded in each section.

FIGURE CAPTIONS

1. B - J Characteristics of Various Hard Superconductors.
    1. Approximate Short Sample Current Densities of Nb_3-Sn (RCA).
    2. Nb (25%) Zr (Supercon).
    3. Nb (22 at %) Ti (A.I.).
    4. Nb (48%) Ti (Supercon old wire).
    5. Nb (48%) Ti (Supercon new wire).
    6. Nb (48%) Ti Cable: 3 supercond: 0.05 cm diameter, 16 copper wires with 0.05 cm diameter, 50 cm long (Supercon).
    7. Nb (22 at %) Ti (A.I.) new cable.
2. Thermal Conductivity of Nb (25%) Zr.
3. Proposed SLAC 1.3 m, 70 kG Liquid Hydrogen Bubble Chamber Magnet.
4. Various Types of Stabilized Superconducting Conductors.
5. Various Proposed Types of Hollow Superconductors.
6. Superconducting Bending Magnet.
7. Comparative Focusing Costs (acc. Smith and Haskill).
    1. Iron Cored Quadrupole.
    2. Superconducting Quadrupole (no iron).
    3. Superconducting Solenoids (no iron).

8a. Magnet Charging Circuit (Used for the SLAC 30.5 cm Magnet).

8b. Magnet Control Circuit (Used for the SLAC 30.5 cm Magnet).

9. SLAC 30.5 cm, 75 kG Helmholtz Coil.
10. Voltage Current Oscillograms for the SLAC 30.5 cm, 75 kG Magnet Cables. At present, four coil sections are being tested.
11. SLAC Superconducting Magnet Installations.
12. 30.5 cm Coil and Dewar Assembly.

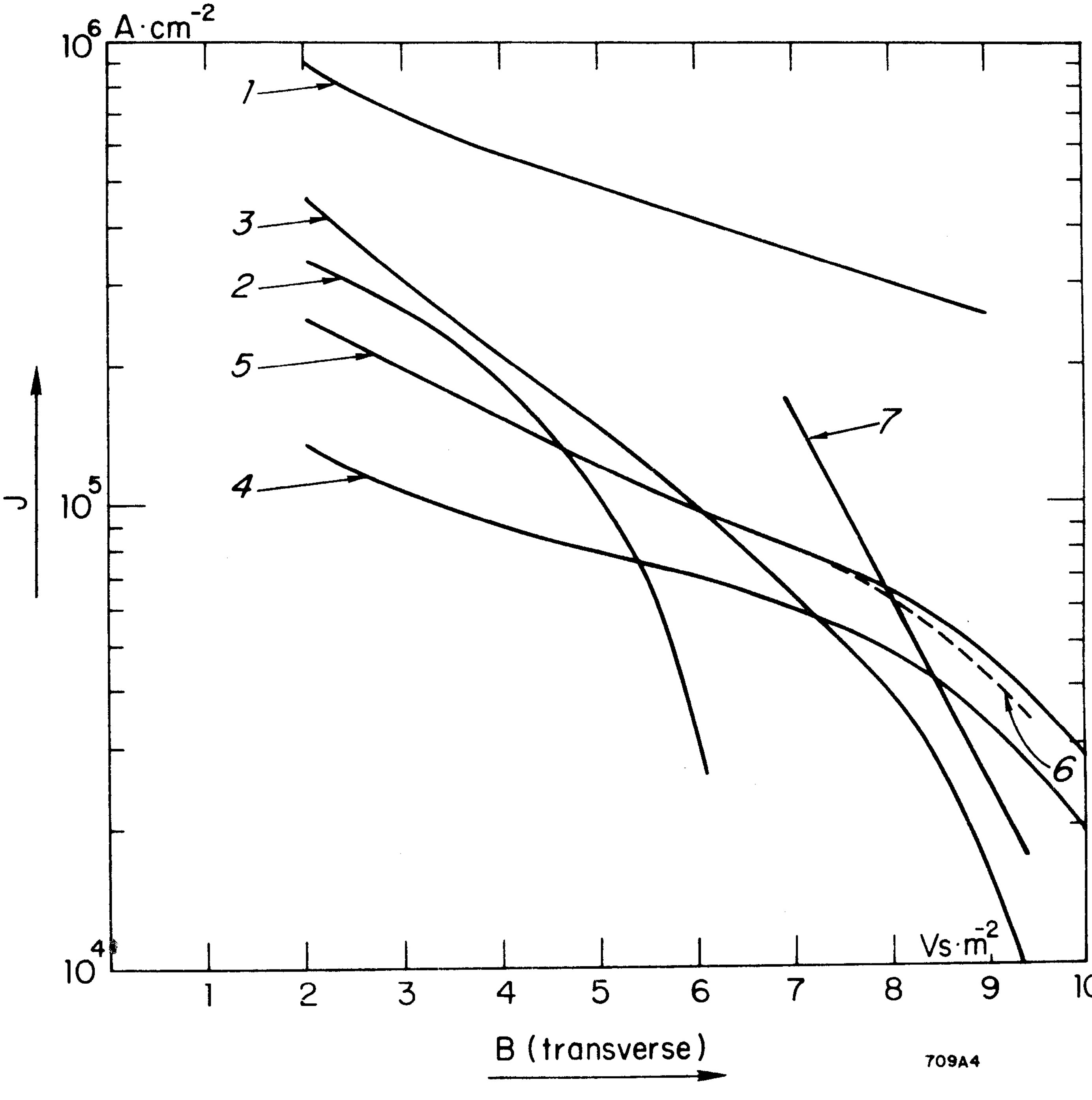

10^6 A·cm^-2
1
3
2
5
4
7
6
J
10^5
10^4
Vs·m^-2
1
2
3
4
5
6
7
8
9
10
B (transverse)
709A4

Fig. 1

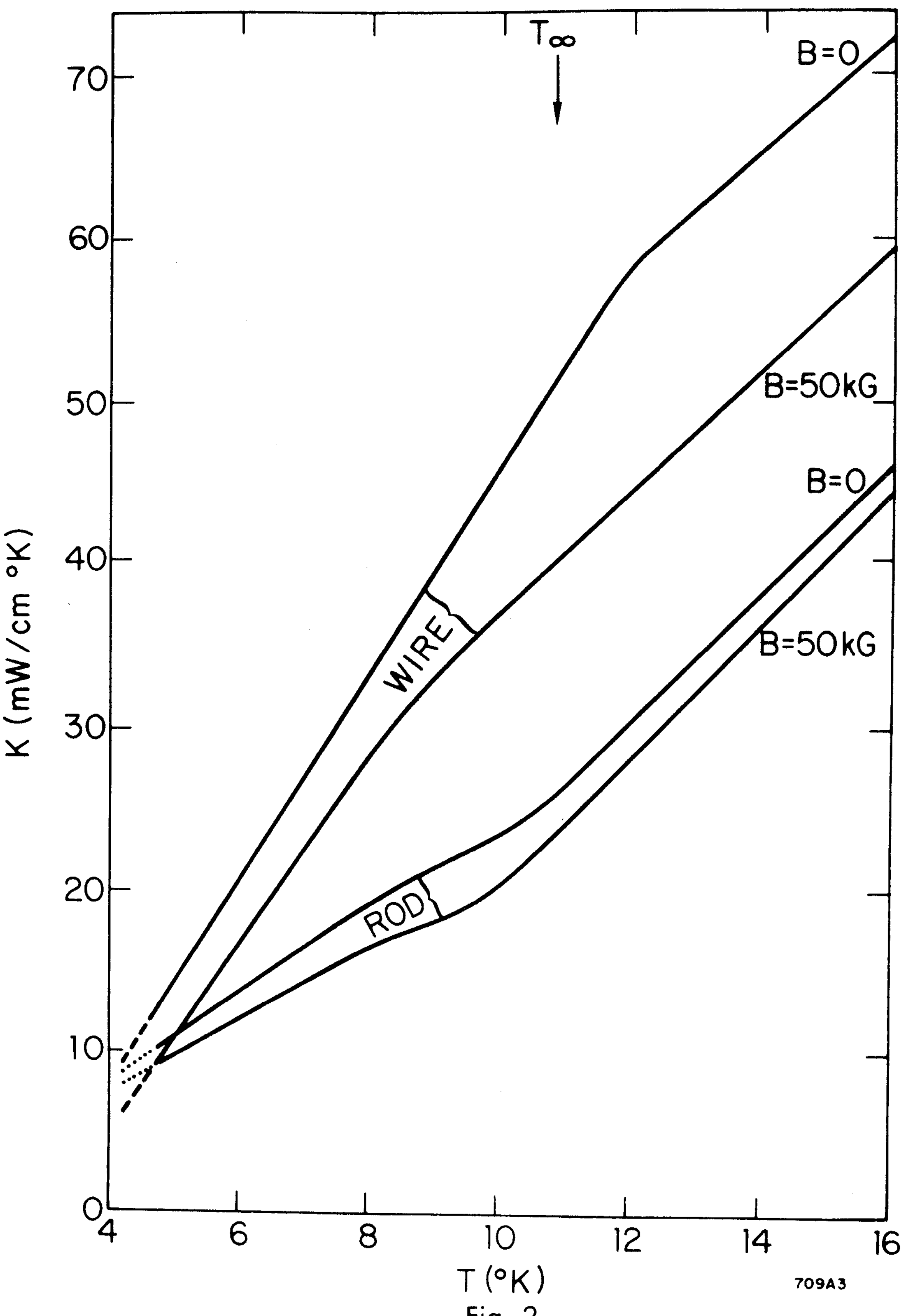

T_∞
B=0
B=50kG
B=0
B=50kG
WIRE
ROD
K (mW/cm °K)
0
10
20
30
40
50
60
70
4
6
8
10
12
14
16
T (°K)
709A3

Fig. 2

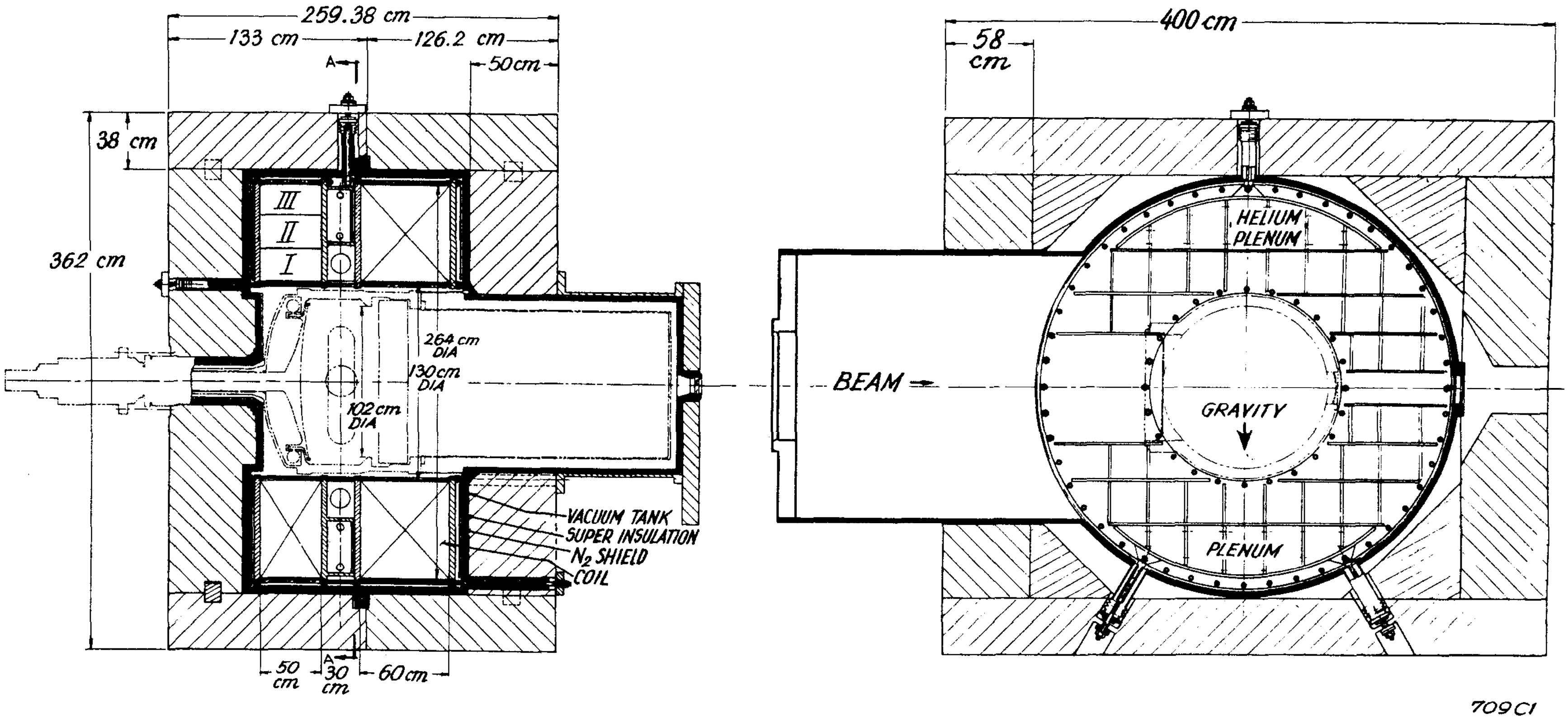
259.38 cm
133 cm
126.2 cm
50cm
A
38 cm
362 cm
III
II
I
264 cm
DIA
130cm
DIA
102cm
DIA
VACUUM TANK
SUPER INSULATION
N_2 SHIELD
COIL
50
cm
30
cm
60cm
400 cm
58
cm
HELIUM
PLENUM
BEAM
GRAVITY
PLENUM
709C1

Fig. 3

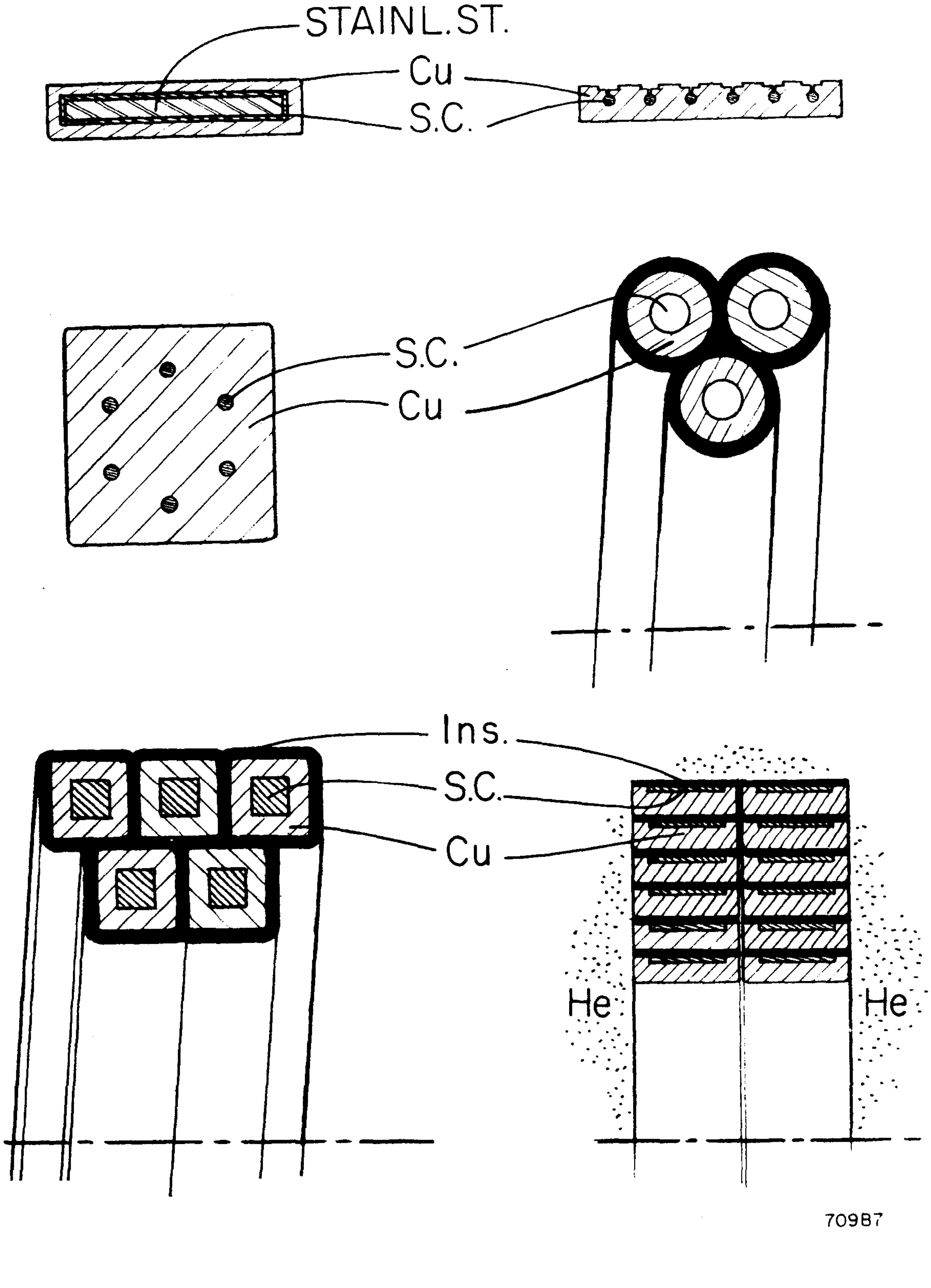

Fig. 4

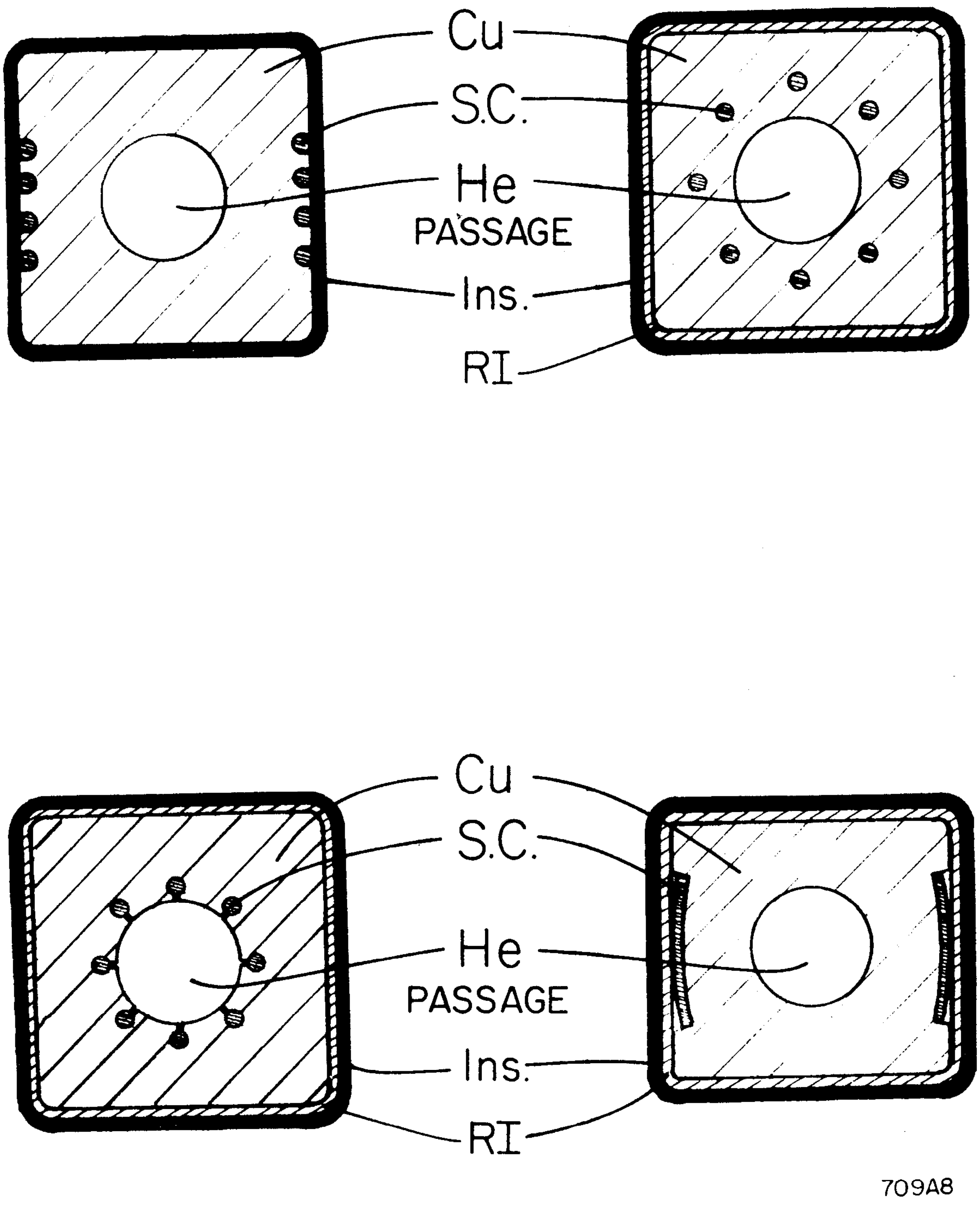

Fig. 5

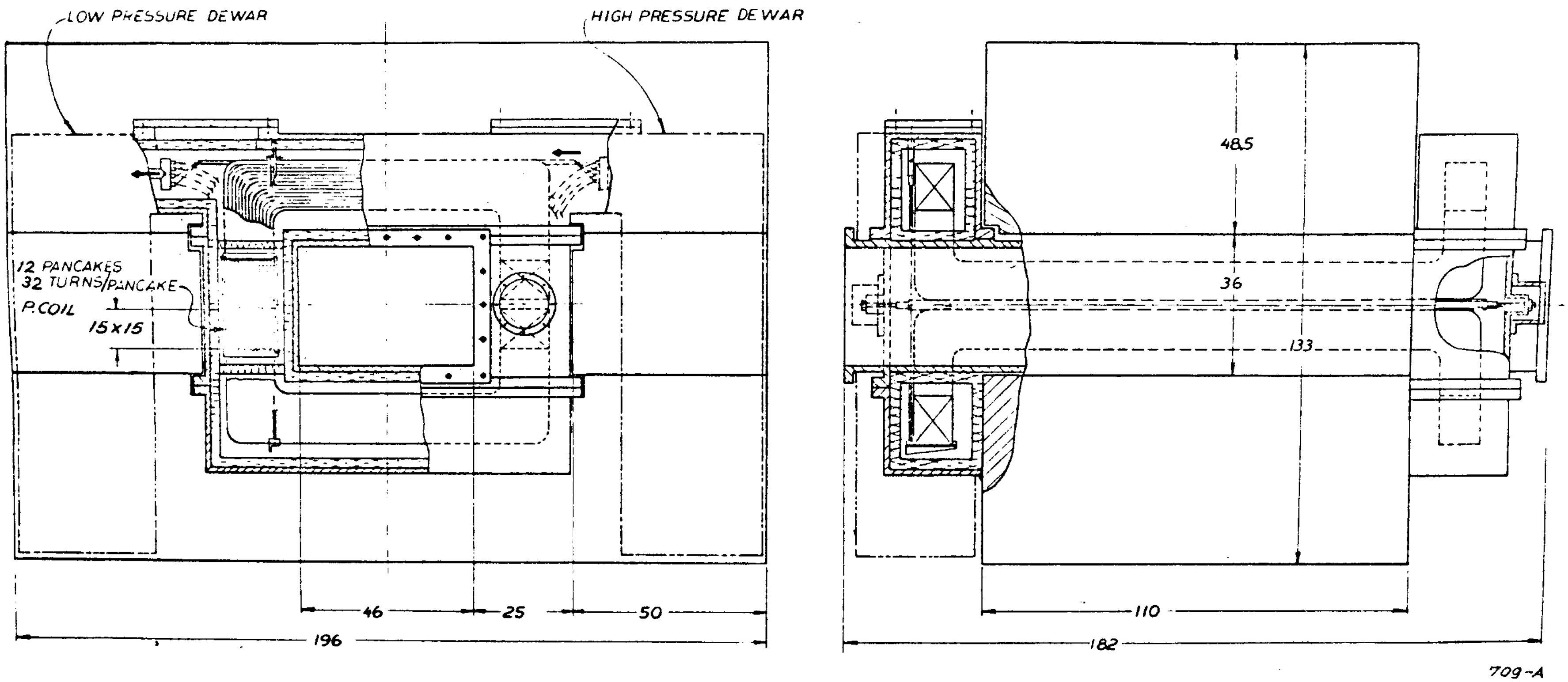

SUPERCONDUCTIVE BENDING MAGNET
Dimensions in Centimeter

Fig. 6

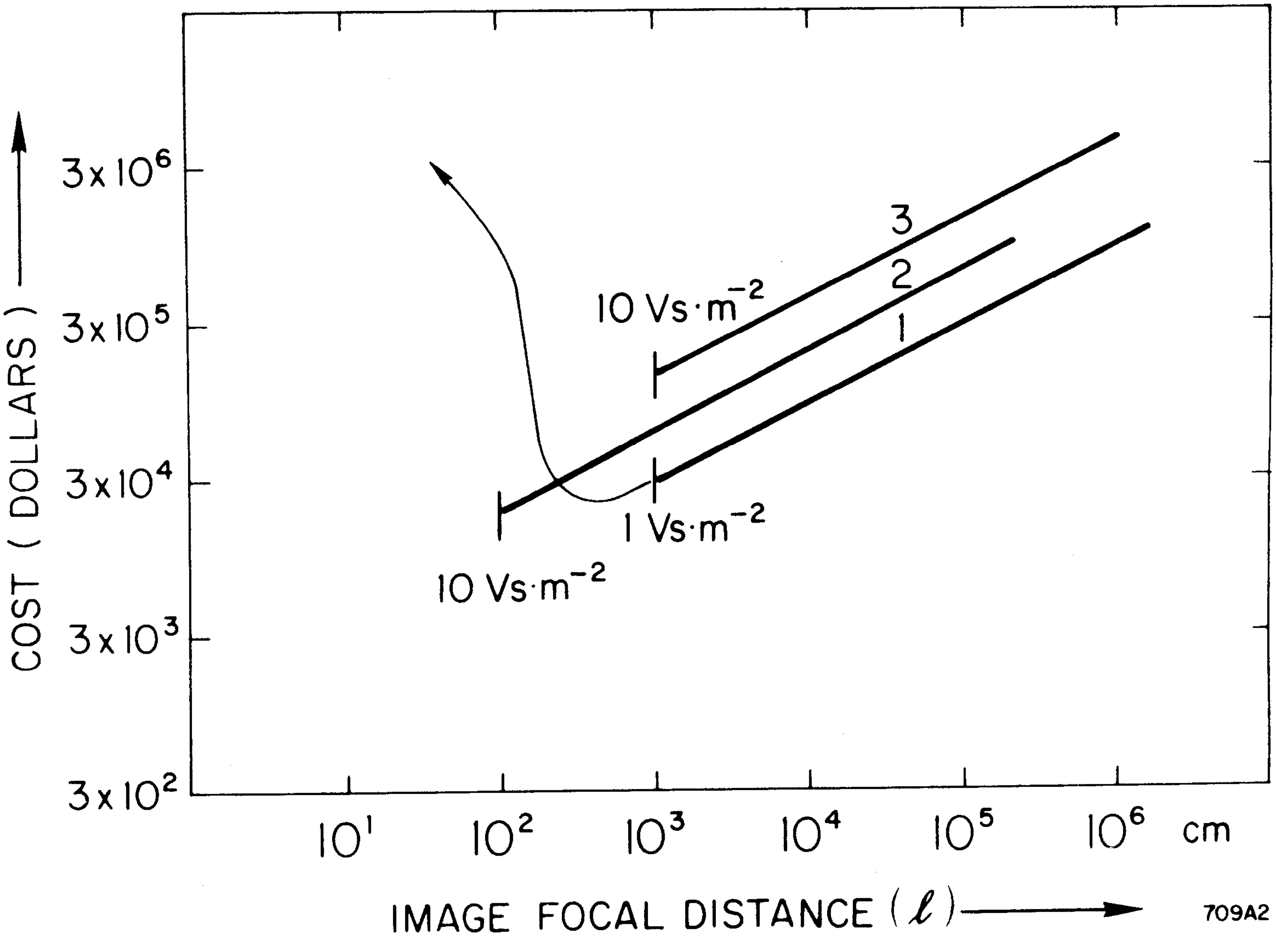

COST (DOLLARS)
3 x 10^6
3 x 10^5
3 x 10^4
3 x 10^3
3 x 10^2
10^1
10^2
10^3
10^4
10^5
10^6 cm
IMAGE FOCAL DISTANCE (ℓ)
3
2
1
10 Vs·m^-2
1 Vs·m^-2
10 Vs·m^-2
709A2

Fig. 7

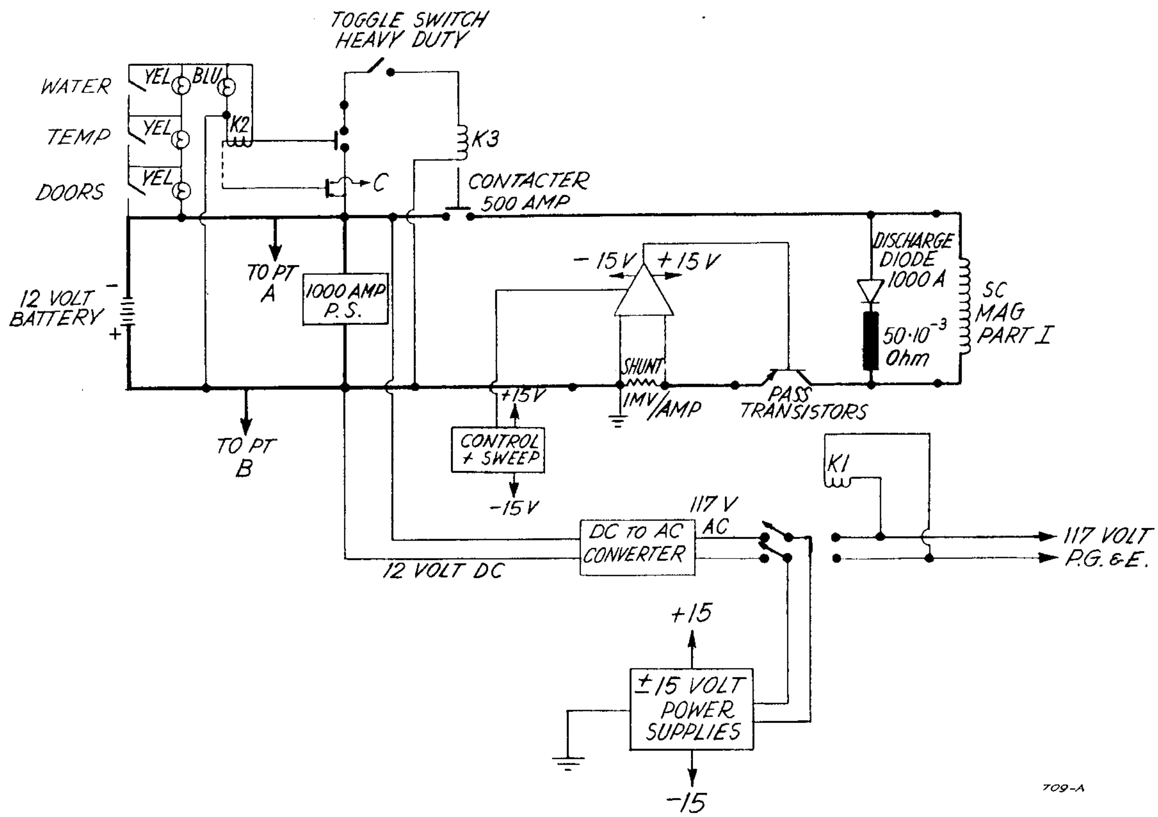
TOGGLE SWITCH
HEAVY DUTY
WATER
TEMP
DOORS
YEL
BLU
YEL
YEL
K2
K3
C
CONTACTER
500 AMP
12 VOLT
BATTERY
TO PT
A
1000 AMP
P.S.
- 15 V
+15 V
DISCHARGE
DIODE
1000 A
SC
MAG
PART I
50·10^-3
Ohm
SHUNT
1MV/AMP
+15V
PASS
TRANSISTORS
TO PT
B
CONTROL
+ SWEEP
-15 V
K1
117 V
AC
DC TO AC
CONVERTER
12 VOLT DC
117 VOLT
P.G.&E.
+15
±15 VOLT
POWER
SUPPLIES
-15
709-A

Fig. 8a

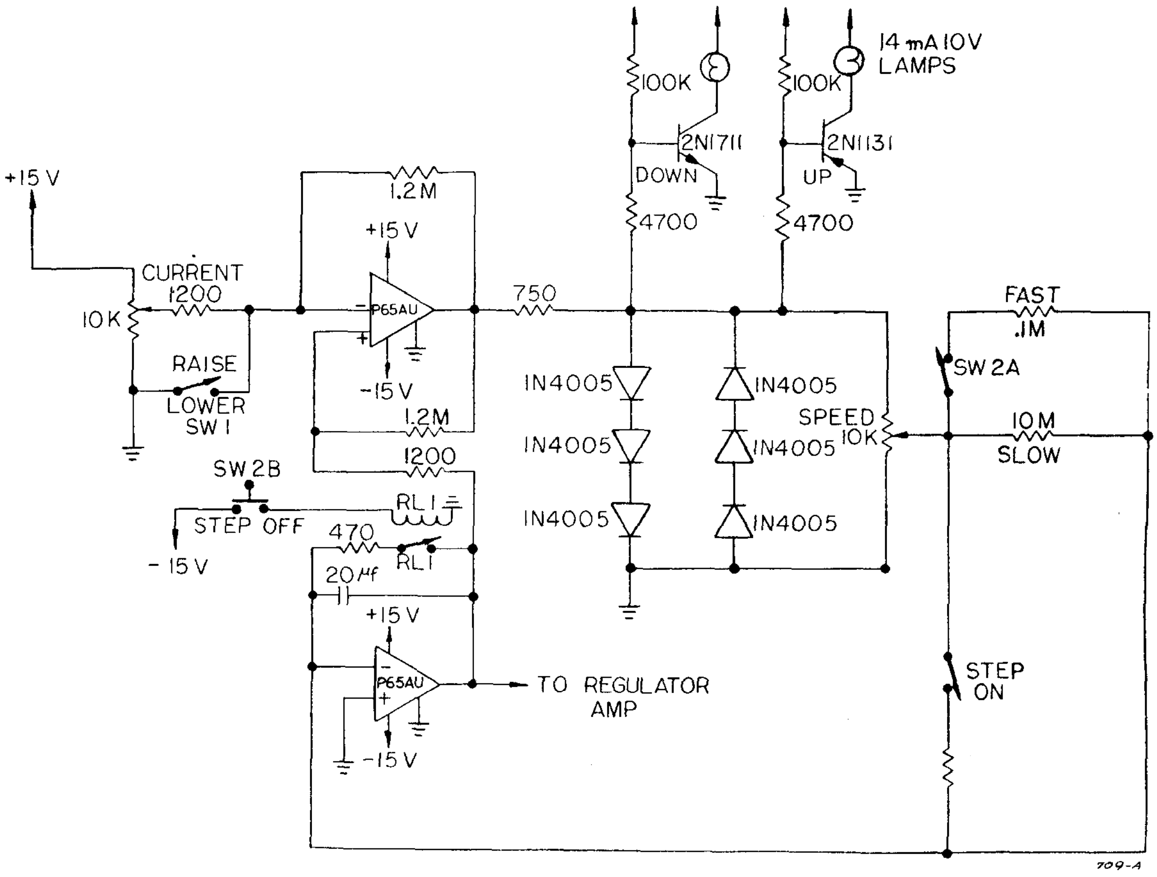
14 mA 10V
LAMPS
100K
100K
2N1711
2N1131
DOWN
UP
4700
4700
+15 V
1.2 M
+15 V
CURRENT
1200
10 K
P65AU
750
FAST
.1M
RAISE
LOWER
SW 1
-15 V
1.2M
1N4005
1N4005
1N4005
1N4005
1N4005
1N4005
SW 2A
SPEED
10K
10 M
SLOW
SW 2B
1200
RL 1
STEP OFF
-15 V
470
RL 1
20 μf
+15 V
P65AU
TO REGULATOR
AMP
-15 V
STEP
ON
709-A

Fig. 8b

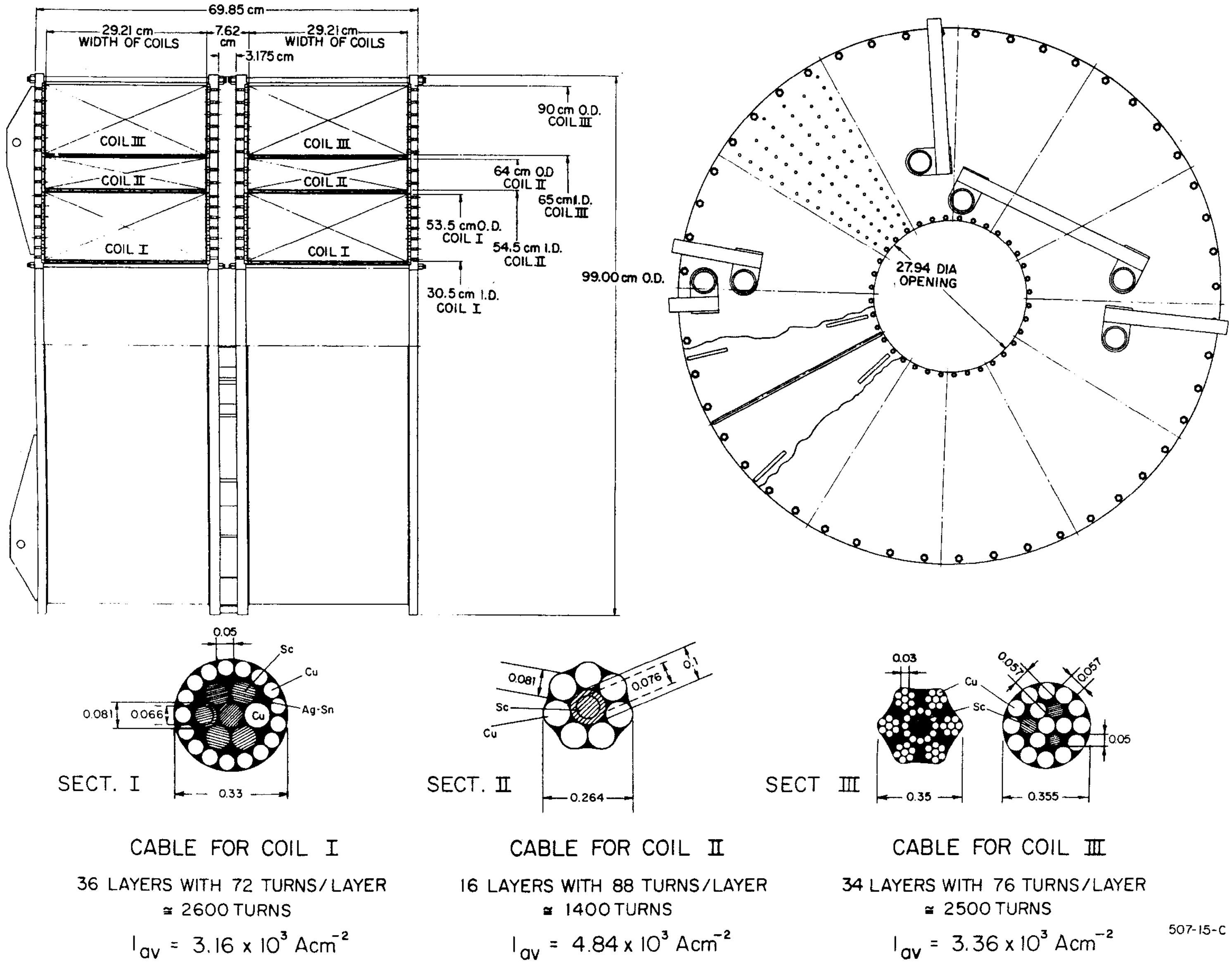

69.85 cm
29.21 cm WIDTH OF COILS
7.62 cm
29.21 cm WIDTH OF COILS
3.175 cm
COIL III
COIL II
COIL I
90 cm O.D. COIL III
64 cm O.D COIL II
65 cm I.D. COIL III
53.5 cm O.D. COIL I
54.5 cm I.D. COIL II
30.5 cm I.D. COIL I
99.00 cm O.D.
27.94 DIA OPENING
0.05
Sc
Cu
Ag-Sn
0.081
0.066
SECT. I
0.33
0.081
0.076
0.1
SECT. II
0.264
0.03
0.057
0.057
0.05
SECT III
0.35
0.355
CABLE FOR COIL I
36 LAYERS WITH 72 TURNS/LAYER
≅ 2600 TURNS
$I_{av} = 3.16 \times 10^3\ Acm^{-2}$
CABLE FOR COIL II
16 LAYERS WITH 88 TURNS/LAYER
≅ 1400 TURNS
$I_{av} = 4.84 \times 10^3\ Acm^{-2}$
CABLE FOR COIL III
34 LAYERS WITH 76 TURNS/LAYER
≅ 2500 TURNS
$I_{av} = 3.36 \times 10^3\ Acm^{-2}$
507-15-C

Fig. 9

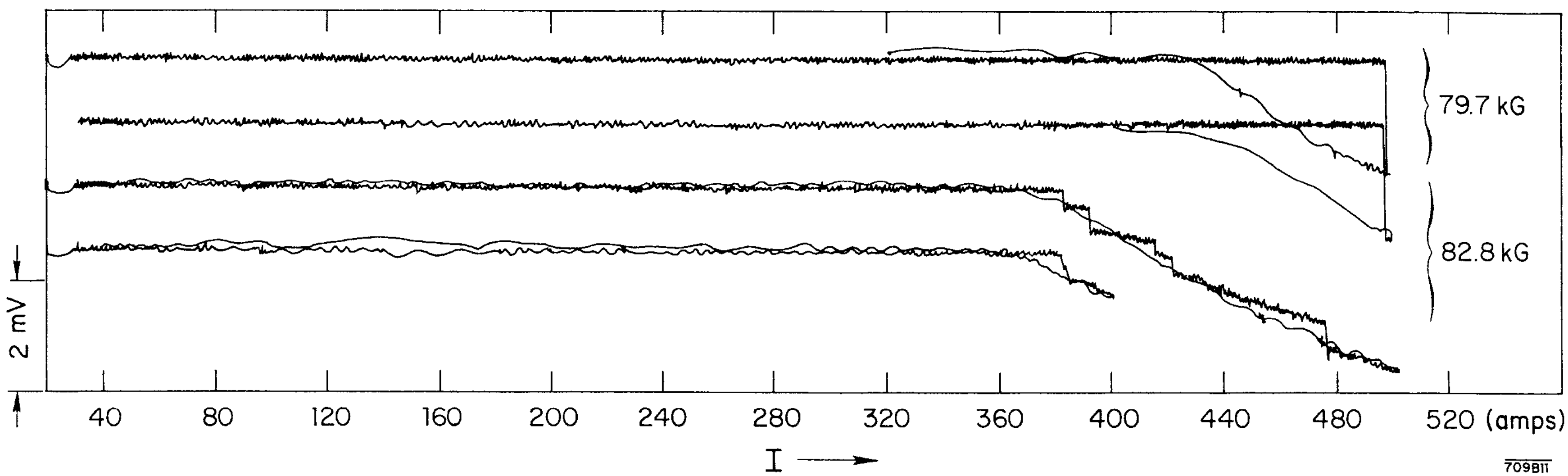

79.7 kG
82.8 kG
2 mV
40
80
120
160
200
240
280
320
360
400
440
480
520 (amps)
I
709B11

Fig. 10

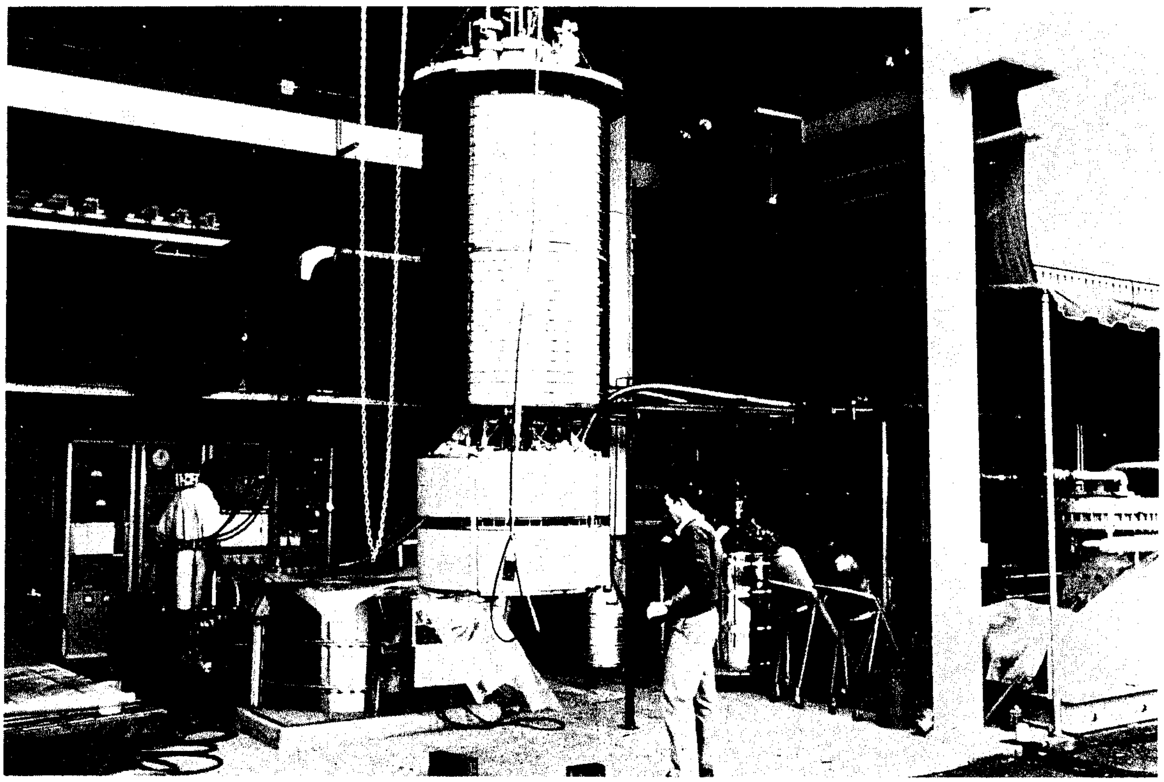

Fig. 11

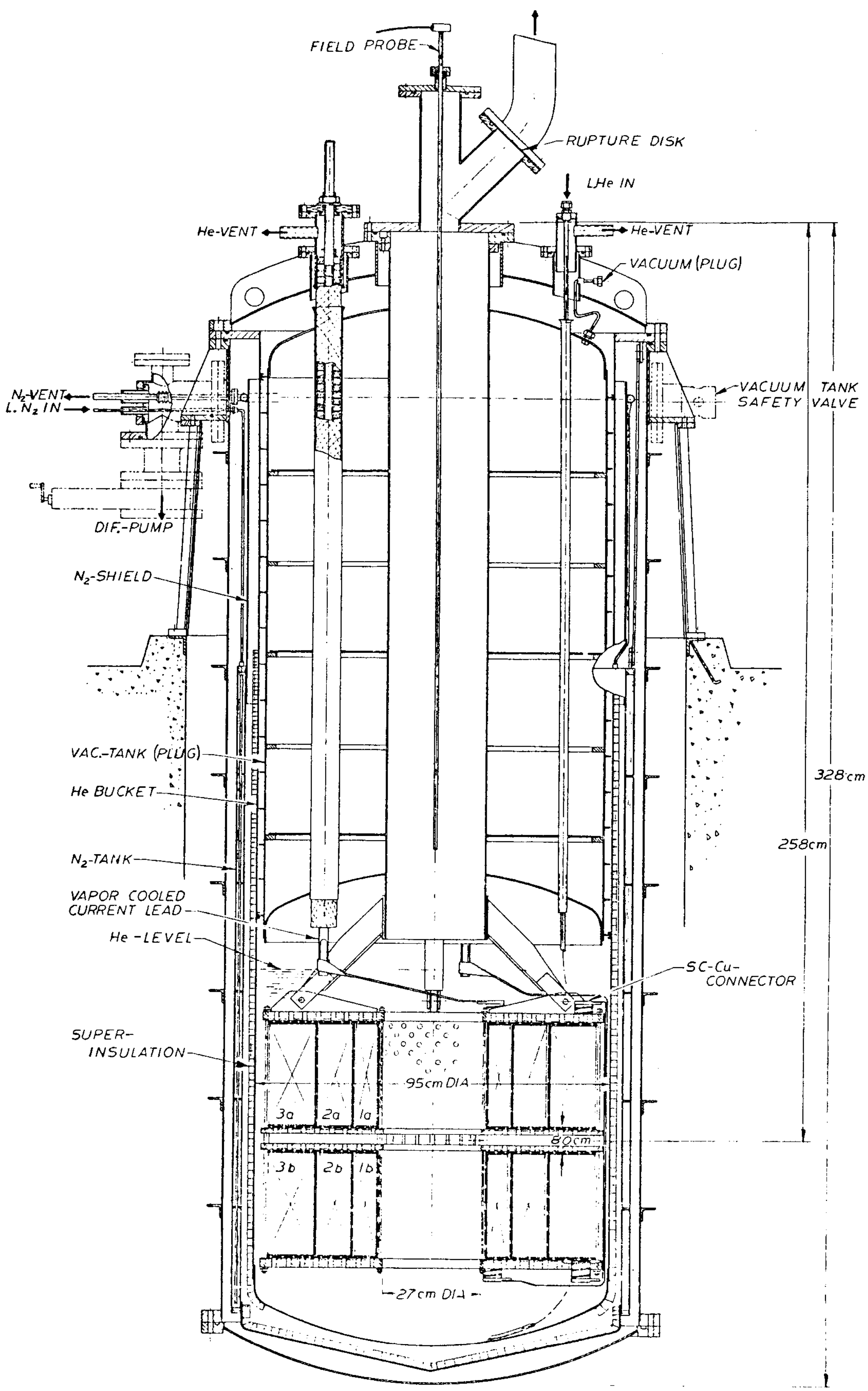

FIELD PROBE
RUPTURE DISK
LHe IN
He-VENT
He-VENT
VACUUM (PLUG)
N_2-VENT
L. N_2 IN
VACUUM TANK
SAFETY VALVE
DIF.-PUMP
N_2-SHIELD
VAC.-TANK (PLUG)
He BUCKET
328 cm
258cm
N_2-TANK
VAPOR COOLED
CURRENT LEAD
He -LEVEL
SC-Cu-
CONNECTOR
SUPER-
INSULATION
95cm DIA
3a
2a
1a
80cm
3b
2b
1b
27cm DIA

Fig. 12